IEEE Photonics Journal
An IEEE Photonics Society Publication

Detection of Calcium-Induced Morphological Changes of Living Cells Using Optical Traps

Volume 2, Number 5, October 2010

A. R. Moradi, Member, IEEE
M. K. Ali
M. Daneshpanah, Member, IEEE
A. Anand
B. Javidi, Fellow, IEEE

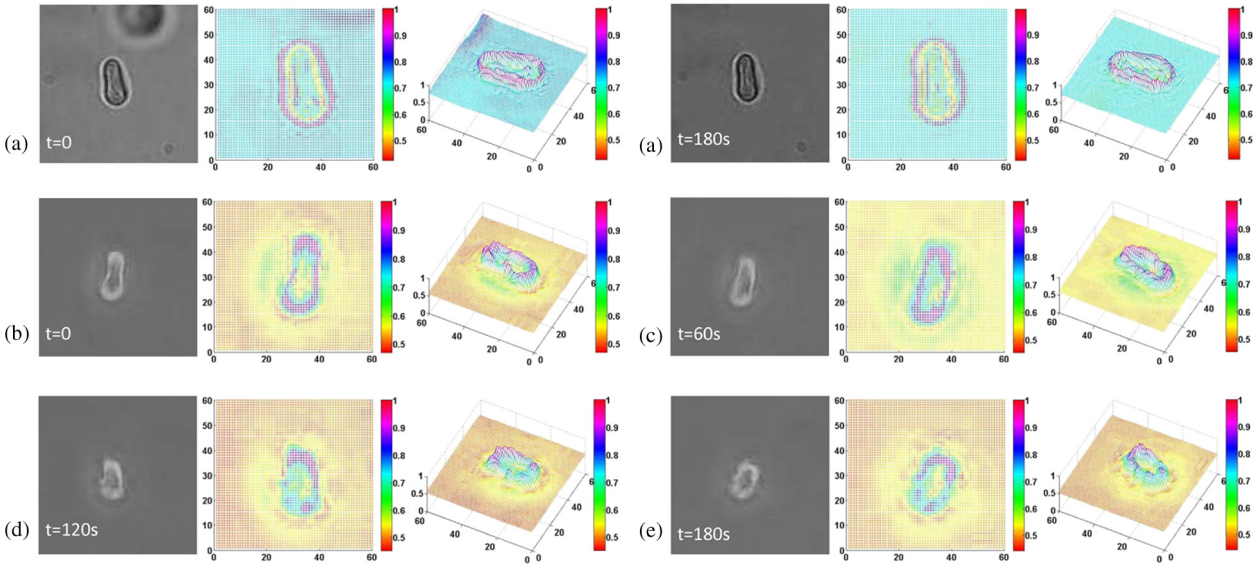

DOI: 10.1109/JPHOT.2010.2068283
1943-0655/$26.00 ©2010 IEEE

IEEE photonics SOCIETY

IEEE

Detection of Calcium-Induced Morphological Changes of Living Cells Using Optical Traps

A. R. Moradi,[1,3] *Member, IEEE*, M. K. Ali,[2] M. Daneshpanah,[4] *Member, IEEE*, A. Anand,[5] and B. Javidi,[4] *Fellow, IEEE*

[1]Department of Physics, Institute for Advanced Studies in Basic Sciences, Zanjan 45195-1159, Iran
[2]Department of Biochemstry and Biophysics, Institute for Advanced Studies in Basic Sciences, Zanjan 45195-1159, Iran
[3]Department of Physics, Zanjan University, Zanjan 45195-313, Iran
[4]Electrical Engineering Department, University of Connecticut, Storrs, CT 06269-2157 USA
[5]Applied Physics Department, Faculty of Technology and Engineering, Maharaja Sayajirao University of Baroda, Vadodara 390001, India

DOI: 10.1109/JPHOT.2010.2068283
1943-0655/$26.00 ©2010 IEEE

Manuscript received June 30, 2010; revised August 9, 2010; accepted August 11, 2010. Date of publication August 17, 2010; date of current version September 3, 2010. Corresponding author: B. Javidi (e-mail: bahram.javidi@uconn.edu).

Abstract: In this paper, we investigate an optical-trap-based method for the detection of structural changes of the red blood cell (RBC) membrane affected by Ca^{2+} ions. Individual cells are immobilized by the use of optical tweezers and are monitored live, while the concentration of Ca^{2+} ions in the buffer is changed simultaneously. Ca^{2+} ions are known to affect the cells' membrane morphology. These changes are attributed to the formation of calcium-induced hydrophobic aggregates of phospholipid molecules in the RBC membrane, resulting in a net change in membrane rigidity. Membrane deformation results in the change of effective radius and the drag coefficient of the cell, both of which affect the Brownian motion of the cell in solution. This motion is indirectly measurable by monitoring the forward scattering light and its dependence on the size and drag coefficient of the cell. We show the relationship between the Ca^{2+} ion concentration and the optical trap specifications. The results are in agreement with previous biological studies and the phase contrast observations of living RBCs under investigation.

Index Terms: Laser micromanipulation, microscopy, blood or tissue sensing, light-tissue-cell interaction.

1. Introduction

Optical tweezers have proven to be a versatile research tool since their inception in the 1980s [1] and have been applied in fundamental research in physics and biology [2], [3]. In biology, optical tweezers provide an elegant approach to immobilize, manipulate, move, and cut microsized biological samples, such as cells [4], chromosomes [5], and DNA molecules [6] in suspension without physical contact and with minimal invasiveness.

An increasing number of investigations are using live cell imaging and tracking techniques to provide critical insight into the fundamental nature of cellular and tissue function. For instance, integration of optical tweezers with available live cell-imaging systems provides advanced tools for many behavioral investigations [7], [8].

In this paper, we use changes in optical trap parameters, such as the corner frequency of the cell's Brownian motion, due to the morphological alteration of trapped cells to monitor the effects of Ca^{2+} ions on the cell membrane. Human RBC is used as a model to observe the calcium-induced morphological changes of the membrane.

RBCs have a relatively simple structure that precludes complexities associated with nucleated cell types [9]. This, among other factors, makes RBC a suitable model for quantitative and analytical studies. In addition, RBC deformations are of extreme importance as they are closely related to important diseases including Malaria and sickle cell anemia [10], [11]. Therefore, the structure and mechanical properties of RBCs have been the topic of detailed investigations for many decades [12], [13]. In recent years, the optical tweezer has proven to be a useful technique for various investigations on RBC mechanics and its visco-elastic characteristics [14]–[20].

Calcium is an essential constituent in biological systems and can affect biological membranes and their properties among other critical roles [21]–[23]. In particular, calcium can affect the shape and size of the cell [24], cell fusion [25], and hemolysis [26]–[28], among others.

In the presented work, the concentration of Ca^{2+} ions is increased by infusing $CaCl_2$ into an RBC bath media (150-mM NaCl). Meanwhile, the corner frequency of the RBCs' Brownian motion, which is shown to be in connection with the membrane rigidity, is measured for samples of different Ca^{2+} ion concentrations by tracking the forward scattering light from the trapped cell.

In Section 2, the sample preparation protocol and the setup used to perform the experiments along with the power spectrum method to track the trapped object and measure trap specification are explained. In Section 3, the experimental results of membrane morphological changes and the calculated corner frequencies are presented. These results are discussed in Section 4, and the paper is concluded in Section 5.

2. Methodology

2.1. Sample Preparation

Freshly collected human blood was obtained from the Blood Bank of Zanjan. Blood was centrifuged at 3000 g for 10 min at 4 °C. Plasma and buffy coat were removed by careful aspiration, and cells were then resuspended in a buffer containing 150-mM NaCl. The cells were then washed three more times with the same buffer. After each centrifugation, the surface of the pellet was thoroughly aspirated. The washed cells were diluted with the same buffer to obtain a 0.1% hematocrit value, making it suitable for single-cell trapping experiments. The samples were kept in water bath maintained at 37 °C before the experiments.

$CaCl_2$ solution was prepared separately in a 10-mM concentration. For each corner frequency measurement, the Ca^{2+} in the chamber was increased in a constant rate by infusing $CaCl_2$ directly into the chamber through a syringe pump. Thus, a specific amount of RBC normal buffer was replaced by $CaCl_2$ and kept for a minute to mix before measurement.

2.2. Setup

The setup (see Fig. 1) provides three functions: optical trapping, $CaCl_2$ chamber and infusion pump, as well as means to track the forward scattered light from the trapped cell. A collimated polarized laser (1064 nm, Compass/2000, Coherent) beam is expanded through a 10X beam expander (BE) and sent to the microscope (IX71, Olymus) port equipped with 1064-nm dichroic mirror. After passing through the microscope objective (100X, phase contrast, oil immersion, NA $= 1.3$, Olympus), the beam is focused to form a stable optical trap. The illuminated sample is imaged through the same objective on a charged coupled device (CCD, SCC-B2013P, Samsung) mounted on the exit port of the microscope. The objective is adjusted so that the trap is formed at the height of 10 μm from the inner surface of the chamber. This would ensure that one can safely ignore the influence of hydrodynamic friction caused by the proximity of the cell and chamber surfaces in calculation of corner frequency [29]. The syringes containing $CaCl_2$ in NaCl and NaCl are attached to the infusion pump motor in opposite directions allowing a push–pull infusion at the

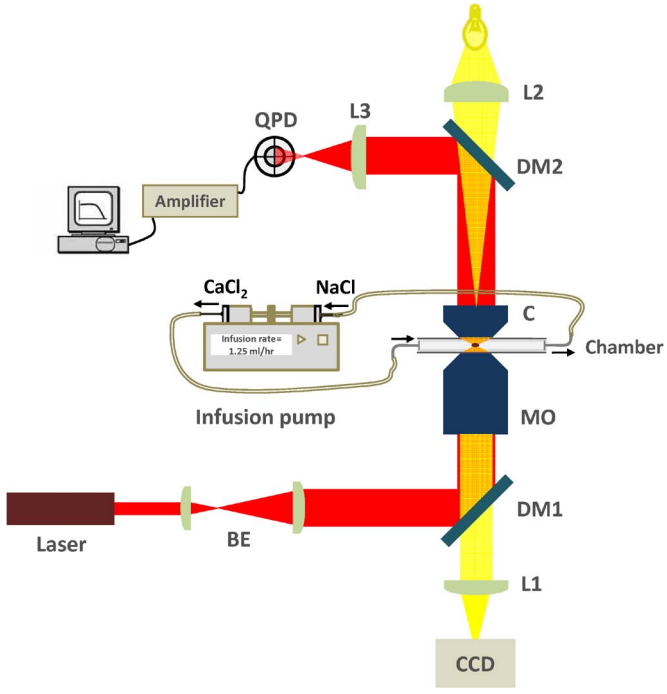

Fig. 1. Schematic of the setup (not to scale). The infusion pump draws $CaCl_2$ into the chamber until that $CaCl_2$ concentration in bath media reaches approximately 5 mM. Simultaneously, the pump withdraws NaCl from the chamber at the same rate. L1, L2, and L3 are lenses, C is a condenser, and DM1 and DM2 are 1064-nm dichroic mirrors to divert the laser beam for trapping and for forward-scattered light tacking, respectively. QPD is a quadrant photodiode which is placed in the conjugate plane of the back focal plane of the condenser, and BE is a 10X beam expander. Signals from QPD are amplified by an amplifier and sent to a computer for analysis.

same flow rate. The volume of the chamber is maintained at 1.5×10^{-7} m^3 throughout the experiment. The chamber consists of a microscope slide and a coverslip equipped with injection tips. The chamber is sealed with vacuum grease to prevent evaporation of the sample.

Phase contrast objective is used for imaging, as it provides high-contrast images of our specimens. In the present setup, the same objective is used to focus the trapping beam as well as to image the sample.

The illumination light is focused on the sample by condenser (C) that is positioned over the sample, while the image of the trapped cell is obtained by the CCD.

The forward scattered light from the trapped cell is collected by the microscope condenser and projected onto a quadrant photodiode (QPD) in order to track the Brownian motion of the trapped cell. A dichroic mirror (DM2) diverts the laser from the imaging path, and the QPD is placed in a plane conjugate to the back focal plane of the condenser.

2.3. Power Spectrum Analysis

Once a cell is trapped, its relative position to the optical axis can be measured in terms of the QPD signal. QPD measures the position as a combination of voltages from its four quadrants. To a reasonable approximation, QPD measurements are proportional to variation in the position of the trapped particle [30]. The resulting signals are amplified and digitized through an A/D converter for further analysis.

For small displacements from the laser focus, the optical potential well formed by the optical beam along the axis x and y, perpendicular to the laser propagation axis, can be considered as a harmonic oscillator. In particular, for a nonspherical particle, like an RBC, the potential shape due to small displacements can be approximated with a parabola [31].

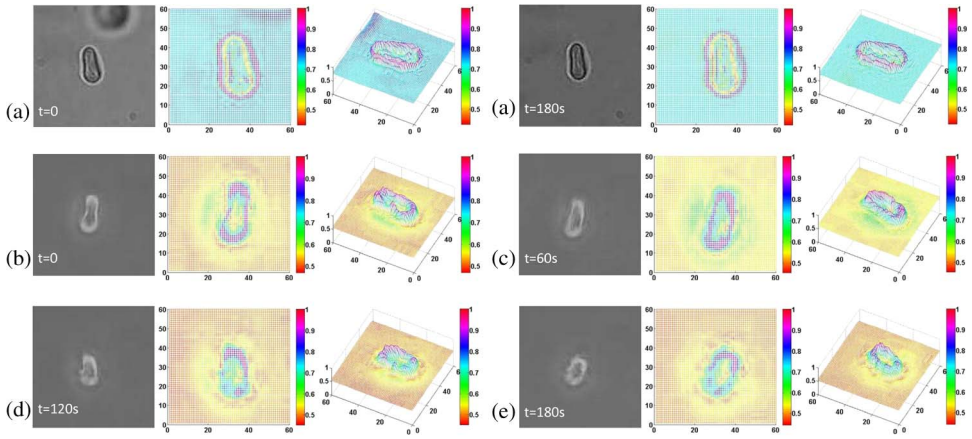

Fig. 2. CCD image and corresponding 3-D profile of optically trapped cell in different times after exposure to $CaCl_2$. (a) The cell is trapped with a laser power of 892 mW; to confirm that the morphological changes are induced by environmental changes, no $CaCl_2$ was drawn for this case into the chamber, and the cell only remained trapped for 180 s. The first and second snaps correspond to the beginning of the experiments $(t = 0)$ and the end $(t = 180\ s)$, respectively. In (b)–(e), the cell was trapped by laser power of 244 mW, and $CaCl_2$ was drawn at a rate of 1.25 ml/h. (b) The trapped cell before $CaCl_2$ infusion. (c)–(e) The trapped cell when exposed to an infusion of $CaCl_2$ for 60-s, 120 s, and 180 s, respectively. Each time, the infusion is followed by a 60-s switching of the pump. The concentration of $CaCl_2$ is approximately 1.3 mM, 2.6 mM, and 3.9 mM, respectively, in the solution.

The stochastic signal derived from the Brownian motion of the trapped cell can be analyzed in the frequency domain. The power spectrum of the Brownian motion is a stochastic function, similar to the cell position, and can be fitted with its theoretical expectation value. According to the solution of the Lengevin equation in Einstein–Ornstein–Uhlenbeck theory for Brownian motion, for each Cartesian coordinate, the power spectrum of the Brownian motion for a trapped particle is given by the Lorentzian function [32]

$$P(f_x) = \frac{\kappa_B T}{\pi^2 \gamma} \frac{1}{f_x^2 + f_{cx}^2} \tag{1}$$

$$P(f_y) = \frac{\kappa_B T}{\pi^2 \gamma} \frac{1}{f_y^2 + f_{cy}^2} \tag{2}$$

where T is the temperature of the sample, κ_B is the Boltzmann constant, and f denotes the frequency.

One parameter which can be determined from the power spectrum is the corner frequency f_c. The corner frequency is related to the trap stiffness as

$$f_x = \frac{\kappa_x}{2\pi\gamma}, \qquad f_y = \frac{\kappa_y}{2\pi\gamma} \tag{3}$$

where κ_x and κ_y are the trap stiffness along the x and y directions. γ is the drag coefficient. Stokes law describes the drag coefficient of a spherical particle to be $\gamma = 6\pi\eta a$, where η is the fluid viscosity and a the radius of the optically trapped particle. Generally, drag coefficient is determined by dimensional analysis and is a function of the object shape, Reynolds number, and particle to fluid density and the frequency of tumbling [33]. However, for many cases, drag coefficient is only a function of the particle shape. According to the calcium-induced morphological changes of the trapped RBCs in our experiments, we are expecting a change in drag coefficient and, hence, in corresponding corner frequencies as the variations are a function of Ca^{2+} concentration in the medium.

The induced morphological changes lead to a change in both the trap stiffness and the drag coefficient. The RBC in normal environment is symmetrically shaped as shown in Fig. 2(a), and it can fill up the focal region with its maximum volume. Hence, the trap is stiff. However, if the RBC undergoes morphological changes from symmetric to asymmetric, the trap stiffness decreases [see

Fig. 2(c)–(e)] because the asymmetric shaped cell cannot cover the maximum space in the focal region.

We have an explanation of how calcium ions can change the symmetric morphology of RBC to asymmetric. This is because calcium is known to interact with phosphatidylserine (PS), which is predominated in the inner layer of bilayer RBC membrane. As PS is negatively charged, they are rarely flipped from the inner layer to the outer layer of the RBC membrane. However, interaction of calcium with PS neutralizes the negative charge, thereby making it easy for PS to flip from the inner layer, pass through the hydrophobic core, and, finally, land on the outer layer of the membrane. It is now widely accepted that the increased presence of PS on the outer layer could induce morphological changes and ultimately cell lysis. It is shown that there is an increased presence of PS on the outer layer in nucleated cells which are undergoing apoptosis [34].

Similarly human erythrocytes are known to undergo certain morphological alterations resembling apoptosis because of the presence of apoptotic enzyme caspase-3 and -8 which are activated by an increase of cytosolic calcium. These enzymes are responsible for the degradation of the RBC cytoskeleton (which is responsible for maintaining normal RBC morphology) [35]. In addition, the change of stiffness can be also ascribed to the variation of ratio between the refractive index of the cell and the buffer, which is caused by the presence of Ca^{2+} ions. It is convenient to use the corner frequency as it reflects both of the aforementioned phenomena.

3. Experimental Results

As shown in Fig. 2, objects shaped like RBC usually try to align themselves with the beam axis in order to find the maximum volume of trapping region [15]. We trapped a single RBC stably at a laser output power of 244 mW and imaged it simultaneously through a phase contrast objective onto the CCD.

While the illuminator is switched off, the motion data is acquired by the QPD. The data acquisition is repeated for laser powers of 460 mW, 676 mW, and 892 mW. In the second step, the pump is turned on for 60 s to increase Ca^{2+} concentration in the RBC chamber. Also, in order to prevent the effect of residual flow on QPD measurements, as well as to allow cells to be incubated long enough with Ca^{2+} ions, the sample is left for 60 s before the next measurement. The measurements are again performed for the above four laser powers. Same procedure is repeated for two more times.

The samples are prepared in 37 °C, and the experiments are conducted at room temperature, i.e., 25 °C. The duration of each experiment is up to 10 min. It has been shown that for temperatures within 25–37 °C, the deformability of RBC is negligible [48]. This is confirmed by our control experiment [see Fig. 2(a)], in which there is no significant morphological changes to the RBC due to the change of the medium temperature.

Images of the cell in presence of different concentrations of Ca^{2+} ions are shown in Fig. 2. In order to confirm that the morphology of the cells are changed due to the presence of Ca^{2+} ions and not due to the heat induced by laser beam [36], a control experiment is conducted in which an RBC is trapped at the highest optical power used (892 mW) and kept for more than 180 s. The phase-contrast snapshots at $t = 0$ and $t = 180$ s, as well as the corresponding intensity profiles, are shown in Fig. 2(a). An insignificant difference in cell shape in this case confirms that the observed morphological changes in other experimental conditions are due to Ca^{2+} ions. Fig. 2(b)–(e) shows an RBC at different times (trapped using laser power of 244 mW) from the beginning of infusion, $t = 0$ [see Fig. 2(b)], in which no Ca^{2+} ion were present in the buffer, at $t = 120$ s [see Fig. 2(c)], $t = 240$ s [see Fig. 2(d)], and $t = 360$ s [see Fig. 2(e)], when the concentration of $CaCl_2$ was approximately 1.3 mM, 2.6 mM, and 3.9 mM in the solution. These concentrations are achieved by flowing $CaCl_2$ for 60 s, 120 s, and 180 s, followed by switching the pump off for 60 s. The phase contrast images of cells [see Fig. 2(b)–(e)] qualitatively show progressive degradation of cell membrane as Ca^{2+} concentration increases.

For quantitative assessment, the QPD signal which contains the information about the position of the trapped cell is amplified and sent to the computer via an analog to digital card. For each case, i.e., each laser power and Ca^{2+} concentration, $N = 10$ data points are acquired. For data processing, we

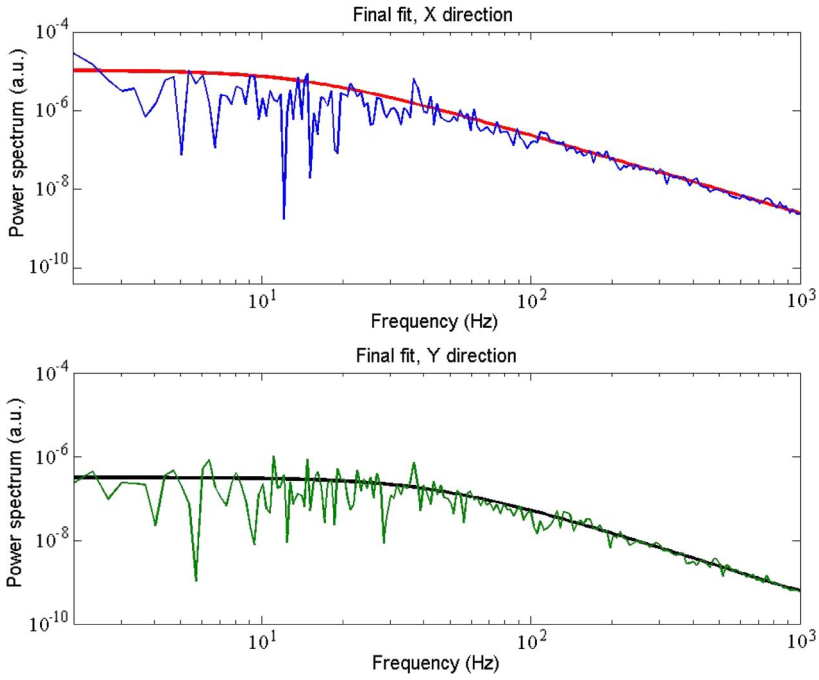

Fig. 3. Power spectrum of a trapped cell and the Lorentzian fitted curve in the *x* and *y* directions.

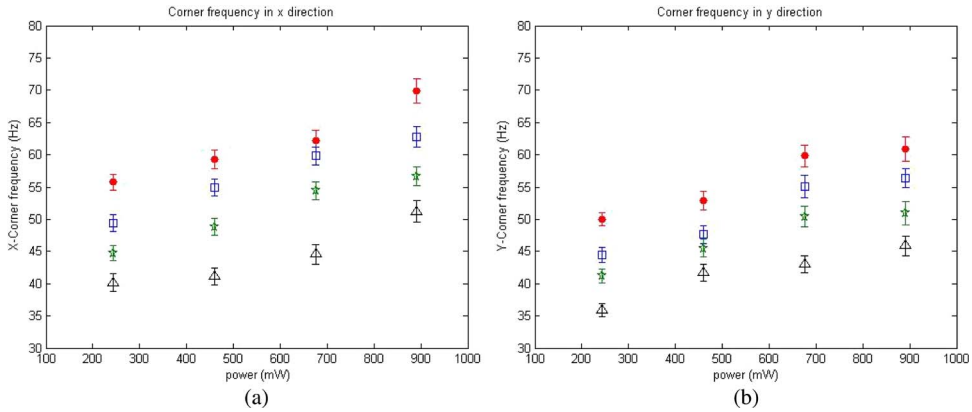

Fig. 4. Calculated corner frequencies in the (a) *x* and (b) *y* directions at different laser intensities. (•) indicates corner frequencies of a trapped cell in its normal environment, (⊓), (⋆), and (△) indicate the samples containing 1.3 mM, 2.6 mM, and 3.9 mM of $CaCl_2$ solution in RBC bath media, respectively.

adapt the method presented by Hansen *et al.* [37]. The sampling frequency is larger than 10 kHz and is sufficiently above the measured corner frequencies. From fitting the Lorentzian equation [see (1) and (2)] to the data in the *x* and *y* directions, the corresponding corner frequencies for each data set can be estimated. The plotted corner frequencies in the *x* and *y* directions are the average of the 10 corner frequencies of the 10 individual data sets. If, in some cases, a strong deviation was found, the measurement was rejected. Fig. 3 shows typical power spectrum of Brownian motion of a trapped RBC and the corresponding fitted Lorentzian curve in the *x* and *y* directions.

4. Discussion

The calculated corner frequencies for the following four cases are shown in Fig. 4, which are 1) the normal cell in absence of $CaCl_2$ in RBC bath media; 2) when the concentration of $CaCl_2$ reaches

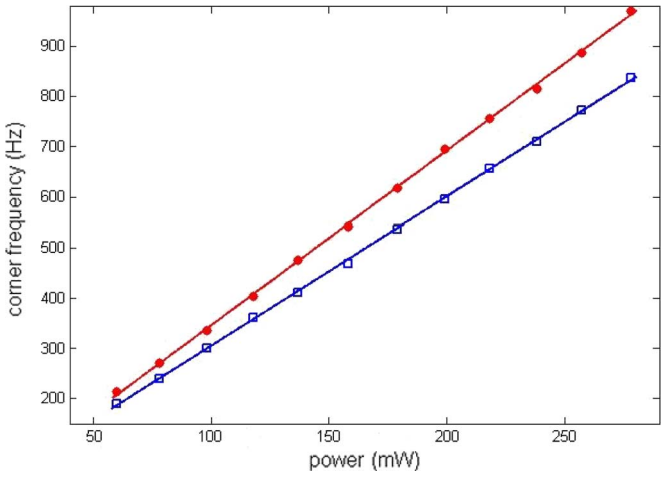

Fig. 5. Dependence of the corner frequencies in x (●) and y (⊓) directions with the laser power for polystyrene bead of 1.09 μm in deionized water.

1.3 mM; 3) 2.6 mM; and 4) 3.9 mM. Fig. 5 shows the dependence of corner frequencies in x and y directions with laser power in the optimized trapping depth. These data are obtained for trapping polystyrene beads of 1.09-μm diameter with the same optical setup. The fact that both x and y corner frequency components have similar values verifies the beam symmetry near the focal point. However, it is generally expected that in the direction of polarization (y direction in our setup), the measured corner frequencies to be obtained slightly smaller than that in the other direction (x direction in our setup). This is due to the asymmetry of the electric field distribution within the trapping region [38]. This difference is smaller when the object is trapped far from the surface.

In Fig. 4, the calculated corner frequencies from four different laser power settings exhibit a strong correlation between the corner frequency and the $CaCl_2$ concentration. For the same incident laser power, the corner frequency is higher for the cells of either the higher refractive index or the smaller size. Note that the linear behavior of the corner frequencies with laser power, as observed with 1.09-μm polystyrene beads, is not present for the RBCs' due to their rather large size and nonrigid structure.

Calcium ions are known to cause aggregations reducing the lateral diffusion of lipid molecules. This, in turn, retards the motion of alkyl chains, which leads to the reduction in the transverse movement of molecules and ions across the aggregates [21]. Ca^{2+} can cause local aggregation of phospholipids bilayers in the membrane, but it causes an overall decrease in the membrane rigidity resulting in greater hemolysis [26]. Therefore, our observation can be interpreted as a result of increased localized aggregation but decreased overall rigidity of phospholipid bilayers in the membrane.

Recently, similar methodology was used to track the changes in the corner frequency of RBC morphology induced by invasion of the malarial parasite [39].

Brownian motion corner frequency of optically trapped cells can be used as a noninvasive way of monitoring structural deformations of individual cells in solution. This noninvasive methodology can be used to study the role of organic components such as cholesterol [40] and sugar [41]. As an increase in the concentration of both of these molecules along with calcium in the blood is associated with development of hypertension, therefore, we expect that the measurement of optical trap parameters of RBC could be exploited in similar diagnostic processes.

In addition, quantitative phase-measurement techniques, such as digital holographic microscopy [42]–[44], can be used to directly observe and model the 3-D morphological changes due to different organic components. This tool has been successfully applied to automatic identification of microorganisms [45], [46] and can be extended to the study of morphological changes in live cells.

It is shown that linearly polarized light induces negligible rotational motion on a normal RBC [47]. Even for Malaria-infected RBCs, the rotational motion is within 0.3 to 5 Hz [47], which is much smaller than the Brownian motion corner frequency range we observe in our experiments. Therefore, the observed decrease in the corner frequency is a result of more pronounced vibrations of the membrane that is due to membrane looseness. Also, for each laser power, the decrease of corner frequencies in the *x* or *y* direction can be attributed to the local rotations of the trapped cell around the axial direction.

5. Conclusion

In conclusion, calcium-ion-induced morphological changes in human RBC is investigated. Optical tweezers are used for cell immobilization and live imaging. Also, the rigidity of a cell membrane is indirectly measured in terms of corner frequency of cells' Brownian motion in different Ca^{2+} concentrations in cell bath media. Our results show that calcium causes overall loosening of the cell membrane, which is in agreement with earlier studies based on induced hemolysis measurement for various kinds of incubations of the cells with calcium. This method can be used to study the effect of other important organic compounds such as cholesterol on structural properties of cells.

Acknowledgment

A. R. Moradi acknowledges stimulating discussions with S. N. S. Reihani and A. Mahmoudi. M. Daneshpanah, A. Anand, and B. Javidi wish to thank F. Schaal and S. Zwick for their useful remarks.

References

[1] A. Ashkin, J. M. Dziedzic, J. E. Bjorkholm, and S. Chu, "Observation of a single-beam gradient force optical trap for dielectric particles," *Opt. Lett.*, vol. 11, pp. 288–290, May 1986.
[2] D. G. Grier, "A revolution in optical manipulation," *Nature*, vol. 424, pp. 810–816, 2003.
[3] C. Bustamante, Z. Bryant, and S. B. Smith, "Ten years of tension: Single-molecule DNA mechanics," *Nature*, vol. 421, pp. 423–427, 2003.
[4] K. Schutze, H. Posl, and G. Lahr, "Laser micromanipulation systems as universal tools in cellular and molecular biology and in cellular and molecular biology and in medicine," *Cell. Mol. Biol.*, vol. 44, no. 5, pp. 747–761, Jul. 1998.
[5] H. Liang, W. H. Wright, S. Cheng, W. He, and M. W. Berns, "Micromanipulation of chromosomes in PTK2 cells using laser microsurgery (optical scalpel) in combination with laser-induced optical force (optical tweezers)," *Exp. Cell Res.*, vol. 204, no. 1, pp. 110–120, Jan. 1992.
[6] M. D. Wang, H. Yin, R. Landick, J. Gelles, and S. M. Block, "Stretching DNA with optical tweezers," *Biophys. J.*, vol. 72, no. 3, pp. 1335–1346, Mar. 1997.
[7] A. Wozniak, J. van Mameren, and S. Ragona, "Single-molecule force spectroscopy using the NanoTracker optical tweezers platform: From design to application," *Curr. Pharm. Biotech.*, vol. 10, no. 5, pp. 467–473, Aug. 2009.
[8] F. Schaal, M. Warber, S. Zwick, H. van der Kuip, T. Haist, and W. Osten, "Marker-free cell discrimination by holographic optical tweezers," *J. Eur. Opt. Soc.—Rapid Publ.*, vol. 4, p. 09 028, Jun. 2009.
[9] E. L. Elson, "Cellular mechanics as an indicator of cytoskeletal structure and function," *Annu. Rev. Biophys. Chem.*, vol. 17, pp. 397–430, 1988.
[10] S. Suresh, J. Spatz, J. P. Mills, A. Micoulet, M. Dao, C. T. Lim, M. Beil, and T. Seufferlein, "Connections between single-cell biomechanics and human disease states: Gastrointestinal cancer and malaria," *Acta Biomaterialia*, vol. 1, no. 1, pp. 15–30, Jan. 2005.
[11] Y. K. Park, C. A. Best, K. Badizadegan, R. R. Dasari, M. S. Feld, T. Kuriabova, M. L. Henle, A. J. Levine, and G. Popescu, "Measurement of red blood cell mechanics during morphological changes," *Proc Nat. Acad. Sci U.S.A.*, vol. 107, no. 15, pp. 6731–6736, Apr. 2010.
[12] G. Bao and S. Suresh, "Cell and molecular mechanics of biological materials," *Nat. Mater.*, vol. 2, no. 11, pp. 715–725, Nov. 2003.
[13] D. Boal, *Mechanics of the Cell*. Cambridge, U.K.: Cambridge Univ. Press, 2002.
[14] R. R. Huruta, M. L. Barjas-Castro, S. T. O. Saad, F. F. Costa, A. Fontes, L. C. Barbosa, and C. L. Cezar, "Mechanical properties of stored red blood cells using optical tweezers," *Blood*, vol. 92, no. 8, pp. 2975–2977, Oct. 1998.
[15] S. C. Grover, R. C. Gauthier, and A. G. Skirtach, "Analysis of the behavior of erythrocytes in an optical trapping system," *Opt. Express*, vol. 7, no. 13, pp. 533–539, Dec. 2000.
[16] M. Dao, C. T. Lim, and S. Suresh, "Mechanics of the human red blood cell deformed by optical tweezers," *J. Mech. Phys. Solids*, vol. 51, no. 11, pp. 2259–2280, Nov. 2003.
[17] J. Li, M. Dao, C. T. Lim, and S. Suresh, "Spectrin-level modeling of the cytoskeleton and optical tweezers stretching of the erythrocyte," *Biophys. J.*, vol. 88, no. 5, pp. 3707–3719, May 2005.

[18] K. Bambardekar, A. K. Dharmadhikari, J. A. Dharmadhikari, D. Mathur, and S. Sharma, "Measuring erythrocyte deformability with fluorescence, fluid forces, and optical trapping," *J. Biomed. Opt.*, vol. 13, no. 6, p. 064 021, Nov./Dec. 2008.
[19] P. Bronkhorst, G. Streekstra, J. Grimbergen, E. Nijhof, J. Sixma, and G. Brakenhoff, "A new method to study shape recovery of red blood cells using multiple optical trapping," *Biophys. J.*, vol. 69, no. 5, pp. 1666–1673, Nov. 1995.
[20] S. K. Mohanty, K. S. Mohanty, and P. K. Gupta, "Dynamics of interaction of RBC with optical tweezers," *Opt. Express*, vol. 13, no. 12, pp. 4745–4751, Jun. 2005.
[21] S. Ohnishi and T. Ito, "Calcium-induced phase separation in phosphatidylserine-phosphatidylcholine membranes," *Biochem*, vol. 13, pp. 881–887, 1974.
[22] F. Liu, H. Mizukami, S. Sarnaik, and A. Ostafin, "Calcium dependent human erythrocyte stability analysis through atomic force microscopy," *J. Struct. Biol.*, vol. 150, no. 2, pp. 200–210, May 2005.
[23] S. M. Burris, J. W. Eaton, and J. G. White, "Evolution of the role of diacyglycerol in calcium-induced erythrocyte shape change and rigidity," *J. Lab. Clin. Med.*, vol. 96, no. 4, pp. 749–756, 1980.
[24] A. Zaidi, M. T. Khan, M. Mirza, I. Ahmad, and M. Saleemuddin, "Studies on the differential morphological alterations in human and goat erythrocytes against ATP depletion and Ca-induced stresses," *Biochem. Mol. Biol. Int.*, vol. 37, pp. 517–526, 1995.
[25] S. M. Farooqui, R. K. Wali, R. F. Baker, and V. K. Kalra, "Effect of cell shape, membrane deformability and phospholipid organization on phosphate-calcium-induced fusion of erythrocytes," *Biochim. Biophys. Acta*, vol. 904, no. 2, pp. 239–250, Nov. 1987.
[26] M. K. Ali and S. Tayyab, "Calcium-induced bilirubin-dependent hemolysis of human erythrocytes," *Biochim. Biophys. Acta*, vol. 1326, no. 1, pp. 124–130, May 1997.
[27] T. Rose, P. Sebo, J. Bellalou, and D. Ladant, "Interaction of calcium with Bordetella pertussis adenylate cyclase toxin," *J. Biol. Chem.*, vol. 270, no. 44, pp. 26 370–26 376, Nov. 1995.
[28] S. T. Test and J. Mitsuyoshi, "Calcium-loaded erythrocytes have a defect in complement regulation distinct from that resulting from exposure to 2-aminoethylisothiouronium bromide," *Blood*, vol. 86, no. 7, pp. 2799–2806, Oct. 1995.
[29] M. Zhong, J. Zhou, Y. Ren, Y. Li, and Z. Wang, "Rotation of birefringent particles in optical tweezers with spherical aberration," *Appl. Opt.*, vol. 48, no. 22, pp. 4397–4402, Aug. 2009.
[30] F. Gittes and C. F. Schmidt, "Interference model for back-focal-plane displacement detection in optical tweezers," *Opt. Lett.*, vol. 23, no. 1, pp. 7–9, Jan. 1998.
[31] A. C. De Luca, G. Volpe, A. M. Drets, M. I. Geli, G. Pesce, G. Rusciano, A. Sasso, and D. Petrov, "Real-time actin-cytoskeleton depolymerization detection in a single cell using optical tweezers," *Opt. Express*, vol. 15, no. 13, pp. 7922–7932, 2007.
[32] F. Gittes and C. F. Schmidt, "Signals and noise in micromechanical measurements," *Methods Cell Biol.*, vol. 55, pp. 129–156, 1998.
[33] D. B. Simons and F. Senturk, *Sediment Transport Technology: Water and Sediment*. Littleton, CO: Water Resources, 1992.
[34] D. L. Bratton, V. A. Fadok, D. A. Richter, J. M. Kailey, L. A. Guthrie, and P. M. Henson, "Appearance of phosphatidylserine on apoptotic cells requires calcium-mediated nonspecific flip-flop and is enhanced by loss of the aminophospholipid translocase," *J. Biol. Chem.*, vol. 272, no. 42, pp. 26 159–26 165, Oct. 1997.
[35] C. P. Berg, I. H. Engels, A. Rothbart, K. Lauber, A. Renz, S. F. Schlosser, K. Schulze-Osthoff, and S. Wesselborg, "Human mature red blood cells express caspase-3 and caspase-8, but are devoid of mitochondrial regulators of apoptosis," *Cell Death Differ.*, vol. 8, no. 12, pp. 1197–1206, Dec. 2001.
[36] J. Erwin, G. Peterman, F. Gittes, and C. F. Schmidt, "Laser-induced heating in optical traps," *Biophy. J.*, vol. 84, no. 2, pp. 1308–1316, Feb. 2003.
[37] P. M. Hansen, I. M. Tolic-Norrelykke, H. Flyvbjerg, and K. Berg-Sorensen, "tweezercalib 2.1: Faster version of MatLab package for precise calibration of optical tweezers," *Comput. Phys. Commun.*, vol. 175, no. 8, pp. 518–520, Oct. 2006.
[38] D. Ganic, X. Gan, and M. Gu, "Exact radiation trapping force calculation based on vectorial diffraction theory," *Opt. Express*, vol. 12, no. 12, pp. 2670–2675, Jun. 2004.
[39] V. Saraogi, P. Padmapriya, A. Paul, U. S. Tatu, and V. Natarajan, "Changes in spectrum of Brownian fluctuations of optically trapped red blood cells due to malarial infection," *J. Biomed. Opt.*, vol. 15, no. 3, p. 037 003, May/Jun. 2010.
[40] S. Razin and J. G. Tully, "Cholesterol requirement of mycoplasmas," *J. Bacteriol.*, vol. 102, no. 2, pp. 306–310, May 1970.
[41] G. van den Bogaart, N. Hermans, V. Krasnikov, A. H. de Vries, and B. Poolman, "On the decrease in lateral mobility of phospholipids by sugars," *Biophys. J.*, vol. 92, no. 5, pp. 1598–1605, Mar. 2007.
[42] F. Dubois, M.-L. Novella Requena, C. Minetti, O. Monnom, and E. Istasse, "Partial spatial coherence effects in digital holographic microscopy with a laser source," *Appl. Opt.*, vol. 43, no. 5, pp. 1131–1139, Feb. 2004.
[43] Y. Frauel, T. J. Naughton, O. Matoba, E. Tajahuerce, and B. Javidi, "Three-dimensional imaging and processing using computational holographic imaging," *Proc. IEEE*, vol. 94, no. 3, pp. 636–653, Mar. 2006.
[44] P. Ferraro, G. Coppola, S. De Nicola, A. Finizio, and G. Pierattini, "Digital holographic microscope with automatic focus tracking by detecting sample displacement in real time," *Opt. Lett.*, vol. 28, no. 14, pp. 1257–1259, Jul. 2003.
[45] B. Javidi, I. Moon, S. Yeom, and E. Carapezza, "Three-dimensional imaging and recognition of microorganism using single-exposure on-line (SEOL) digital holography," *Opt. Express*, vol. 13, no. 12, pp. 4492–4506, 2005.
[46] I. Moon, M. Daneshpanah, B. Javidi, and A. Stern, "Automated three-dimensional identification and tracking of micro/nanobiological organisms by computational holographic microscopy," *Proc. IEEE*, vol. 97, no. 6, pp. 990–1010, Jun. 2009.
[47] J. Dharmadhikari, S. Roy, A. Dharmadhikari, S. Sharma, and D. Mathur, "Torque-generating malaria-infected red blood cells in an optical trap," *Opt. Express*, vol. 12, no. 6, pp. 1179–1184, Mar. 2004.
[48] N. Nemeth, O. K. Baskurt, H. J. Meiselman, F. Kiss, M. Uyuklu, T. Hever, E. Sajtos, P. Kenyeres, K. Toth, I. Furka, and I. Miko, "Storage of laboratory animal blood samples causes hemorheological alterations: Inter-species differences and the effects of duration and temperature," *Korea-Australia Rheology J.*, vol. 21, no. 2, pp. 127–133, 2009.